

Circle Motion Control of Trirotor UAV via Discrete Output Zeroing

Yasuyuki Kataoka, Kazuma Sekiguchi and Mitsuji Sampei

Abstract—In this paper, a nonlinear controller is designed for an underactuated UAV having three inputs to realize “circle motion”, the motion that the attitude of UAV points to the center of circle while the center of mass moves on a circle orbit. The proposed method is redesigning the time-varying output zeroing controller discretely. This method allows output functions to be kept zero even though output functions are changed. In other words, zero dynamics can be controlled by this method. Finally, numerical simulation shows the validity of the proposed nonlinear controller.

I. INTRODUCTION

UAV is high-potential application that opens up new innovating applications in various fields. The notable property that UAV usually owns is structural underactuation. For example, Quadrotor UAV system[3] has four inputs whereas the degree of freedom is six. One of the challenges of UAV is to find out what motion can be realized via less inputs. Finding answers would suggest restriction of mechanical design and control objective of fail-safe. In this paper, a strongly underactuated UAV system which has only three-inputs is considered. Specifically, Trirotor UAV having only three inputs[1] is considered as an example of controlled object. The main contribution of this paper is to suggest a new nonlinear controller realizing “circle motion” which requires both three dimensional position control and one dimensional attitude control by three inputs. The control method this paper would be useful for fail-safe control strategy in real applications, which is highly required from the perspective of practical usage.

In previous research[1], some characteristics of the suggested Trirotor UAV were revealed. This Trirotor UAV does not have equilibrium point without a condition of model parameter. In addition, this model does not have locally asymptotically stabilizability even though the model satisfies the condition. This result proves the fact that it is impossible to control hovering motion by three inputs via continuous time-invariant state feedback. Reflecting this result, the control objective is set as one of the periodic motions, “circle motion” which is shown in Fig.1. In this paper, “circle motion” is defined as the motion that the center of mass moves on an arbitrary circle orbit while the attitude of UAV points to the center of the orbit. For practical usage, this circle motion allows a camera-mounted UAV to take photo or video for a target in the center of the circle orbit.

Y. Kataoka, K. Sekiguchi, M. Sampei are with the Department of Mechanical and Control Engineering, Tokyo Institute of Technology, 2-12-1 Ookayama, Meguro-ku, Tokyo 152- 8550, Japan kataoka@sc.ctrl.titech.ac.jp, sekiguchi@ctrl.titech.ac.jp, [sampei@ctrl.titech.ac.jp](mailto:sampeim@ctrl.titech.ac.jp)

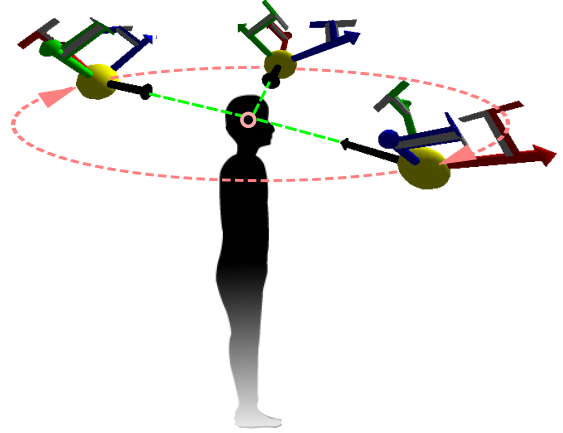


Fig. 1. Image of Circle Motion Control

In this paper, the nonlinear equation for the Trirotor UAV is briefly derived in section II. Note that the proposed Trirotor model owns literally only three inputs, which means this does not own any other input such as servo motors as other Trirotor models have.[4][5] Next, system analysis discusses some characteristics of underactuated Trirotor UAV in section III. The results, especially *Strongly Accessibility*, lead control objective to periodic motion. Then, the control design, the main contribution of this paper, is addressed in section IV. The design method of the discrete output zeroing control for the Trirotor model is mentioned. Numerical simulation confirms the effectiveness of the proposed nonlinear controller. Finally, conclusion and future work are given in section V.

II. MODELING

This section briefly introduces a dynamic model of Trirotor UAV shown in Fig.2 and Fig.3. One of the main features of this model is the three rotors which are installed on three skew axes. One note here is that this model does not own other inputs such as a servo motor to control tilting angle. Here, the behavior of this model is briefly described. As is shown in bold red letters in Fig.2, the rotation of rotor 1 generates the translational force in positive y direction. Plus, this rotation generates two different moments, positive rotation about the axis of y and negative rotation about the axis of z . Consequently, two moments on each axis cancel each other to suppress the attitude variation.

A. Assumption against Trirotor UAV

The model assumptions are given in this section. The details about this model can be found in [1]. In this paper,

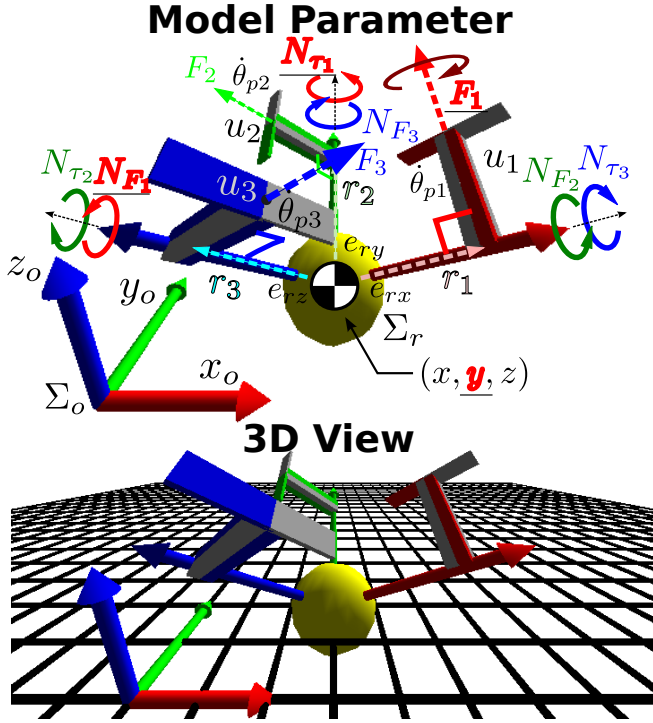


Fig. 2. Overview of UAV Model having Three Rotors

significant assumptions and definitions are briefly introduced.

1) Input to Trirotor UAV

The system inputs to this system are assumed to be torque inputs driven by DC motors which are connected to three rotors.

2) Counteraction against Input Torque

The counteraction against input torque can not be neglected for this system, since the inertia of this vehicle is assumed to be relatively small to the input torque. The moments vector generated by three inputs result in

$$\mathbf{N}_r = \begin{bmatrix} N_{F_2} - N_{\tau_3} \\ N_{F_3} - N_{\tau_1} \\ N_{F_1} - N_{\tau_2} \end{bmatrix} = \begin{bmatrix} (r_2 \times F_{r2}) - u_3 \\ (r_3 \times F_{r3}) - u_1 \\ (r_1 \times F_{r1}) - u_2 \end{bmatrix} \quad (1)$$

TABLE I

PHYSICAL VARIABLES

Σ_o	: inertial coordinate system
Σ_r	: relative coordinate system
ξ	: position of the center of gravity of robot (x, y, z)
η	: posture angle : Euler angle (ϕ, θ, ψ)
ω_0	: angular velocity vector defined on Σ_o
ω_r	: angular velocity vector defined on Σ_r
$\dot{\theta}_{pi}$: angular velocity of i th rotor(propeller)
$\dot{\theta}_p$: vector of $\dot{\theta}_{pi}$, $[\dot{\theta}_{p1}, \dot{\theta}_{p2}, \dot{\theta}_{p3}]^T$
F_{ri}	: force to direction i on Σ_r
F_r	: force vector on Σ_r , $[F_{rx}, F_{ry}, F_{rz}]^T$
N_{Fi}	: moment of force generated by F_i
N_{τ_i}	: counteraction generated by the rotation of rotor i
N_r	: total moment vector on Σ_r
u	: torque input to each motors $[u_3, u_1, u_2]^T$

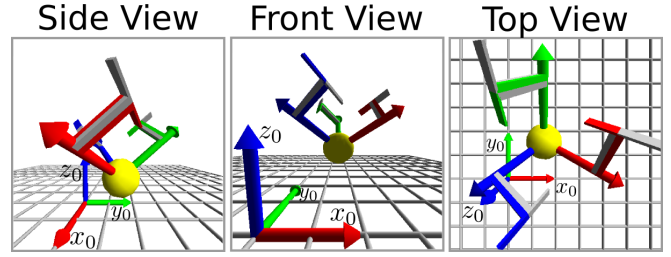


Fig. 3. Trirotor UAV Model from Different Angle

3) Propulsion Force generated by Rotors

Each translational force generated by the three rotors is proportional to square of the angular velocity of the rotors,

$$\mathbf{F}_r = \begin{bmatrix} k_{p3} \text{sgn}(\dot{\theta}_{p3}) \dot{\theta}_{p3}^2 \\ k_{p1} \text{sgn}(\dot{\theta}_{p1}) \dot{\theta}_{p1}^2 \\ k_{p2} \text{sgn}(\dot{\theta}_{p2}) \dot{\theta}_{p2}^2 \end{bmatrix} \quad (2)$$

where k_{pi} denotes the constant parameter representing the property of rotor i .

4) Air Friction caused by Body Rotation

It is also assumed that the air friction caused by body rotation generates viscous term to attitude dynamics. This viscous term physically means the rotation velocity converges, if there remains constant moment to the system.

B. Nonlinear Equation

First, let q_e denote the state of the Trirotor model,

$$q_e = : [\xi^T, \dot{\xi}^T, \eta^T, \dot{\eta}^T, \theta_p^T]^T \in \mathbb{R}^{12} \times \mathbb{S}^3 \quad (3)$$

where each variable is defined in Table I. Note that θ_p can be neglected from system realization because it does not affect system dynamics.

Next, let the coordinate transformation matrices be defined as

$$\omega_r = \mathbf{R}^T(\eta) \omega_0 \quad (4)$$

$$\mathbf{R}(\eta) = \begin{bmatrix} C_\psi C_\theta & -C_\phi S_\psi + C_\psi S_\phi S_\theta & S_\phi S_\psi + C_\phi C_\psi S_\theta \\ C_\theta S_\psi & C_\phi C_\psi + S_\phi S_\psi S_\theta & -C_\psi S_\phi + C_\phi S_\psi S_\theta \\ -S_\theta & C_\theta S_\phi & C_\phi C_\theta \end{bmatrix} \quad (5)$$

$$\omega_r = \mathbf{T}(\phi, \theta) \dot{\eta} \quad (6)$$

$$\mathbf{T}(\phi, \theta) = \begin{bmatrix} 1 & 0 & -S_\theta \\ 0 & C_\phi & S_\phi C_\theta \\ 0 & -S_\phi & C_\phi C_\theta \end{bmatrix} \quad (7)$$

TABLE II

PHYSICAL PARAMETERS

m	: mass of the suggested model
J_r	: inertia tensor defined on Σ_r (constant)
D_r	: viscous matrix by air friction defined on Σ_r
J_p	: $\text{diag}\{J_{p3}, J_{p1}, J_{p2}\}$, J_{pi} : rotary inertia of i th rotor
D_p	: $\text{diag}\{D_{p3}, D_{p1}, D_{p2}\}$, D_{pi} : coefficient of viscosity
k_{pi}	: coefficient of property of i th rotor
r_i	: vector from COG to operating point of F_i on Σ_r
g	: gravitational acceleration

where $S_* = \sin*$ and $C_* = \cos*$ are used for simplification. The dynamics of Trirotor system can be derived via Lagrange-Euler method

$$M\ddot{\xi} = -C_\xi + R(\eta)F_r \quad (8)$$

$$J_r\ddot{\eta} = -C_\eta(\phi, \theta, \dot{\eta}) + T^T(\phi, \theta)N_r \quad (9)$$

$$J_p\ddot{\theta}_p = -C_{\theta_p}(\phi, \theta, \dot{\eta}) + u \quad (10)$$

where C_ξ is constant matrix and $C_\eta(\phi, \theta, \dot{\eta}), C_{\theta_p}(\phi, \theta, \dot{\eta})$ are matrices composed of nonlinear elements. Consequently, the 15 dimensional nonlinear state equation is obtained in state space form by defining

$$\dot{q}_e =: f_e(q_e) + g_e(q_e)u \quad (11)$$

where $f_e(q_e) \in \mathbb{R}^{15 \times 1}, g_e(q_e) \in \mathbb{R}^{15 \times 3}$. The detail of modeling process is in [1].

III. SYSTEM ANALYSIS

In this section, the property of Trirotor model is analyzed to reveal the limitation of control objective. In previous research[1], the significant result regarding *Locally Asymptotically Stabilizability* was revealed. Here, *Strongly Accessibility* is additionally discussed to indicate the feasibility of periodic motion.

A. Equilibrium point

It is verified that there does not exist equilibrium point in Trirotor model (11) unless the model satisfies the specific conditions of model parameters which are discussed in [1].

B. Locally Asymptotically Stabilizability (LAS)

The notion of LAS[2] for UAV system is equivalent to whether hovering control is mathematically possible or not. The result was gained that it is impossible to locally asymptotically stabilize a generic UAV model by time-invariant continuous state feedback control using three inputs even if the system has equilibrium point. This result indicates that hovering control can not be the control objective for three-inputs system.

C. Strongly Accessibility

Let $g_e = [g_{1e}, g_{2e}, g_{3e}]$ denote control input vector field. Plus, let $C_{sa}(q_{e0})$ denote *Strongly Accessibility Distribution*[7]. *Strongly Accessibility Distribution* for this system (11) is equivalent to the involutive closure \bar{G}_{sa} , where G_{sa} is defined as $\text{span}\{g_e, [f_e, g_{ie}], [f_e, [f_e, g_{ie}]], \dots\}$ ($i = 1, 2, 3$) and x_0 is an arbitrary state. Thus, (12) is the condition for system (11) to own *Strongly Accessibility* at a point q_{e0} .

$$\text{rank}(C_{sa}(q_{e0})) = \text{rank}(\bar{G}_{sa}(q_{e0})) = 15 \quad (12)$$

In this section, *Strongly Accessibility distribution* at several states q_{ej} ($j = 1, 2$) are numerically computed because the analytical computation of *Strongly Accessibility* for the Trirotor UAV model (11) is difficult due to the complexity of system model.

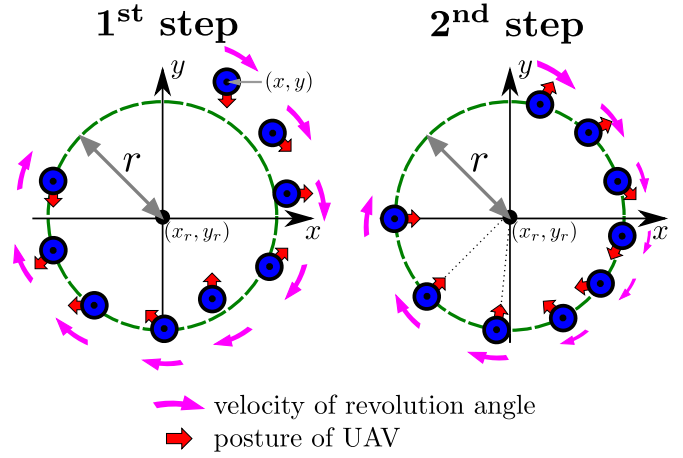


Fig. 4. Image of Control Strategy

- $q_{e1} = [O^{1 \times 3}, O^{1 \times 3}, \frac{\pi}{4}, \tan^{-1}(\frac{1}{\sqrt{2}}), 0, O^{1 \times 3}, 1^{1 \times 3}]^T$
This is the condition that the posture of Trirotor UAV is upward such as in Fig.2 and every propellor has velocity. *Strongly Accessible Distribution* at point q_{e1} results in

$$\text{rank}(C_{sa}(q_{e1})) = 15 \quad (13)$$

. Therefore, the system (11) can be shown to be *Strongly Accessible* at q_{e1} .

- $q_{e2} = [O^{1 \times 3}, O^{1 \times 3}, \frac{\pi}{4}, \tan^{-1}(\frac{1}{\sqrt{2}}), 0, O^{1 \times 3}, O^{1 \times 3}]^T$
This is the almost same condition as above but the velocities of every propellors are zero. *Strongly Accessible Distribution* at point q_{e2} results in

$$\text{rank}(\bar{G}_{sa2}) = 12 \quad (14)$$

where $G_{sa2} = \text{span}\{g_e, ad_f^1 g_{ie}, ad_f^2 g_{ie}, ad_f^3 g_{ie}\}$ and $i = 1, 2, 3$. The numerical computation of Lie bracket in the higher order is not possible due to the complexity. This result infers that there exist singular points that should be avoided in the design of desired trajectory.

Through the analysis of LAS and *Strongly Accessibility*, periodic motions need to be affirmatively considered as a control objective rather than hovering control for Trirotor model (11).

IV. CONTROLLER DESIGN

The control objective of circle motion is defined as motion that the center of mass moves on a circle orbit while the attitude of UAV points to the center of circle. The image of this motion is given in Fig.1. This control objective requires the 3 dimensional position control and 1 dimensional attitude control via 3 inputs, which means controlling zero dynamics is demanded. In this section, we propose a nonlinear control method that enables zero dynamics to be controlled.

A. Formulation of Circle Motion Control

The control strategy can be divided into next two steps.

- 1st step : position control of UAV on a circular orbit
- 2nd step : posture control of UAV pointing the center

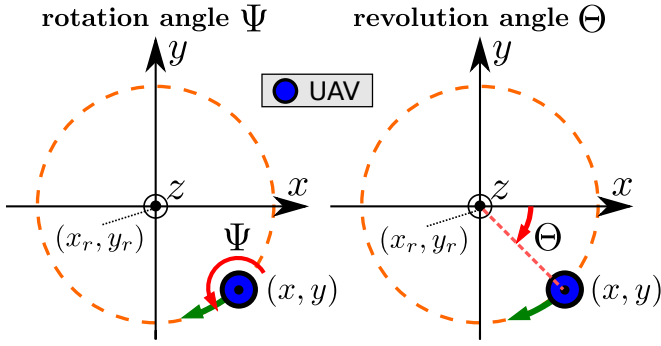


Fig. 5. definition of Ψ and Θ

The image of this step-based control strategy is shown in Fig.4. In the 1st step, the position of COG is controlled via output zeroing in order to let UAV move on an arbitrary circle orbit. Then, in the 2nd step, the posture is controlled so that a desired surface of UAV faces to the center of the circle orbit. The significantly important point of control design in 2nd step is to keep output functions zero in order to control zero dynamics explicitly.

Here, let “rotation angle” and “revolution angle” be introduced for the formulization of the control objective in each steps explicitly. The image of both angle is shown in Fig.5.

Let Ψ denote “rotation angle”, the rotation angle about the axis of z on Σ_0 . The velocity associated with Ψ corresponds to the element z of ω_0 defined in Table I. The representation of Ψ and $\dot{\Psi}$ by euler angle η result in

$$\Psi = \psi \quad (15)$$

$$\dot{\Psi} = -\sin(\theta)\dot{\phi} + \dot{\psi} \quad (16)$$

Note (16) is obtained by from (5) and (7).

Next, let Θ denote “revolution angle”, the rotation angle of the circle orbit on xy -plane. Θ and $\dot{\Theta}$ are determined with position x, y and velocity \dot{x}, \dot{y} by

$$\Theta = \tan^{-1} \left(\frac{y - y_r}{x - x_r} \right) \quad (17)$$

$$\dot{\Theta} = \frac{(x - x_r)\dot{y} + (y - y_r)\dot{x}}{(x - x_r)^2 + (y - y_r)^2} \quad (18)$$

where (x_r, y_r) is the desired center of the target circular orbit. Then, the goal of 1st step is formulized as

$$x \rightarrow x_r + r \cos(\Theta_d(t)) \quad (19)$$

$$y \rightarrow y_r + r \sin(\Theta_d(t)) \quad (20)$$

$$z \rightarrow z_r \quad (21)$$

where $\Theta_d(t)$ is the time-variant function representing the target trajectory of revolution angle Θ and z_r is the desired height.

Next, the goal of 2nd step is interpreted as the correspondence of rotation angle Θ and revolution angle Ψ . Let e and \dot{e} denote the error of these angles. Then, the goal of

2nd step is formulized by (22) and (23).

$$e = \Psi - \Theta \rightarrow 0 \quad (22)$$

$$\dot{e} = \dot{\Psi} - \dot{\Theta} \rightarrow 0 \quad (23)$$

B. Control Design in 1st step

The goal of 1st step is achieved via output zeroing control. The details of the design procedure of output zeroing in MIMO case can be found in [6]. The output functions to realize the goal of 1st step are designed as

$$\mathbf{h} = \begin{bmatrix} h_1 - h_{r1}(t) \\ h_2 - h_{r2}(t) \\ h_3 - h_{r3} \end{bmatrix} = \begin{bmatrix} x - (x_r + r \cos(\Theta_d(t))) \\ y - (y_r + r \sin(\Theta_d(t))) \\ z - z_r \end{bmatrix} \quad (24)$$

where $\Theta_d(t)$ is a linear function of time t . Since all of the relative degree for each of output functions in (24) is 3, the original system can be partially linearized via input-output linearization as 9 dimensional linear subspace. Then, there remains the rest of unobservable 6 dimensional nonlinear subspace. The control input for input-output linearization is designed by

$$\mathbf{u} = -\boldsymbol{\alpha}^{-1}(\mathbf{q}_e) (\boldsymbol{\beta}(\mathbf{q}_e) - \mathbf{v}) \quad (25)$$

$$\boldsymbol{\alpha}(\mathbf{q}_e) = \begin{bmatrix} a_{11} & a_{12} & a_{13} \\ a_{21} & a_{22} & a_{23} \\ a_{31} & a_{32} & a_{33} \end{bmatrix}, \boldsymbol{\beta}(\mathbf{q}_e) = \begin{bmatrix} b_1 \\ b_2 \\ b_3 \end{bmatrix} \quad (26)$$

$$a_{ij} = L_{g_{e_j}} L_{f_e}^2 h_i(\mathbf{q}_e) \quad (27)$$

$$b_i = L_{f_e}^3 h_i(\mathbf{q}_e) - \frac{\partial^3}{\partial t^3} h_{ri}(t) \quad (28)$$

The obtained linear subsystem results in

$$\dot{\boldsymbol{\sigma}} = \mathbf{A}\boldsymbol{\sigma} + \mathbf{B}\mathbf{v} \in \mathbb{R}^{9 \times 1} \quad (29)$$

$$\mathbf{A} = \begin{bmatrix} \mathbf{A}_3 & \mathbf{O}^{3 \times 3} & \mathbf{O}^{3 \times 3} \\ \mathbf{O}^{3 \times 3} & \mathbf{A}_3 & \mathbf{O}^{3 \times 3} \\ \mathbf{O}^{3 \times 3} & \mathbf{O}^{3 \times 3} & \mathbf{A}_3 \end{bmatrix}, \mathbf{A}_3 = \begin{bmatrix} 0 & 1 & 0 \\ 0 & 0 & 1 \\ 0 & 0 & 0 \end{bmatrix} \quad (30)$$

$$\mathbf{B} = \begin{bmatrix} \mathbf{B}_3 & \mathbf{O}^{3 \times 1} & \mathbf{O}^{3 \times 1} \\ \mathbf{O}^{3 \times 1} & \mathbf{B}_3 & \mathbf{O}^{3 \times 1} \\ \mathbf{O}^{3 \times 1} & \mathbf{O}^{3 \times 1} & \mathbf{B}_3 \end{bmatrix}, \mathbf{B}_3 = \begin{bmatrix} 0 \\ 0 \\ 1 \end{bmatrix} \quad (31)$$

$$\boldsymbol{\sigma} = \begin{bmatrix} \sigma_1 \\ \sigma_2 \\ \sigma_3 \end{bmatrix}, \boldsymbol{\sigma}_i = \begin{bmatrix} h_i - h_{ri}(t) \\ L_{f_e} h_i(\mathbf{q}_e) - \frac{\partial}{\partial t} h_{ri}(t) \\ L_{f_e}^2 h_i(\mathbf{q}_e) - \frac{\partial^2}{\partial t^2} h_{ri}(t) \end{bmatrix} \quad (32)$$

by input-output linearization (25). The linear systems (29) is easily controlled by designing $\mathbf{v} \in \mathbb{R}^{3 \times 1}$ using linear control theory unless states (3) are designed to pass the point at which the system (11) does not own *Strongly Accesibility*.

The rest of unobservable nonlinear subsystem by input-output linearization (25) results in

$$\dot{\boldsymbol{\zeta}} = \boldsymbol{\Gamma}(\boldsymbol{\sigma}, \boldsymbol{\zeta}, t) \in \mathbb{R}^{6 \times 1} \quad (33)$$

$$\boldsymbol{\zeta} = [\boldsymbol{\eta}^T, \boldsymbol{\eta}^T]^T \quad (34)$$

where $\boldsymbol{\zeta}$ is chosen so that the coordinate transformation of input-output transformation satisfies *diffeomorphism*.

The nonlinear subsystem (33) is called *Zero Dynamics*, when output zeroing is realized. In this case, zero dynamics is represented by

$$\dot{\boldsymbol{\zeta}} = \boldsymbol{\Gamma}(\mathbf{O}^{9 \times 1}, \boldsymbol{\zeta}, t) \quad (35)$$

. In the second step, it is required to control zero dynamics so that (22) and (23) are satisfied.

C. Control Design in 2nd step

Before the controller design, let some parameter be defined regarding discretization. Let sampling interval denote $k : [t_k, t_{k+1}]$. In addition, let the desired trajectory function of revolution angle at interval k denote $\Theta_d^{\{k\}}(t)$. Moreover, let $\dot{\Theta}_d^{\{k\}}(t_{k+1}) = \frac{d}{dt}\Theta_d^{\{k\}}(t_{k+1})$ denote the desired velocity of revolution angle at $t = t_{k+1}$ in interval k . This parameter will be a design parameter for a discrete controller. In the 2nd step, the controller (25) becomes discrete output zeroing controller by using these parameters.

The main idea of the control strategy in 2nd step is to modify $\Theta_d(t)$ in (24) discretely. The challenges of this control are mainly next two points:

- (a) preservation of output zeroing against discretization,
- (b) design of discontinuous controller.

First, let challenge (a) be argued. In order to preserve the achievement of 1st step, it is necessary to maintain the continuity of output functions and the derivatives of them until the third time derivative, because the relative degrees of output functions are all 3. Otherwise, there occurs deviation from the desired circular motion which is achieved in the 1st step. Plus, the first time derivative of desired trajectory, $\dot{\Theta}_d^{\{k\}}(t)$, should monotonically increase or decrease at interval k . Overall, these conditions require $\Theta_d^{\{k\}}(t)$ to satisfy the following 7 equations.

- I $\Theta_d^{\{k\}}(t_k) = \Theta(t_k)$
- II $\dot{\Theta}_d^{\{k\}}(t_k) = \dot{\Theta}(t_k)$
- III $\ddot{\Theta}_d^{\{k\}}(t_k) = 0$
- IV $\dddot{\Theta}_d^{\{k\}}(t_k) = 0$
- V $\ddot{\Theta}_d^{\{k\}}(t_{k+1}) = 0$
- VI $\dddot{\Theta}_d^{\{k\}}(t_{k+1}) = 0$
- VII $\int_{t_k}^{t_{k+1}} \ddot{\Theta}_d^{\{k\}}(t) dt = \frac{\dot{\Theta}_d^{\{k\}}(t_k) + \dot{\Theta}_d^{\{k\}}(t_{k+1})}{2}$

The conditions of I ~ IV are initial conditions, and V and VI are the conditions for assurance of continuity. The condition VII is the one for $\dot{\Theta}_d^{\{k\}}(t)$ to reach desired $\dot{\Theta}_d^{\{k\}}(t_{k+1})$ at time $t = t_{k+1}$ monotonically. Note that it is unnecessary to control $\Theta_d^{\{k\}}(t_{k+1})$, the revolution angle at $t = t_{k+1}$, in 2nd step.

Hereby, $\Theta_d^{\{k\}}(t)$, the desired trajectory function of revolution angle at interval k , can be found as sixth-order polynomial denoted by

$$\Theta_d^{\{k\}}(t) = \sum_{l=0}^6 p_l t^l \quad (36)$$

where, $p_l (l = 0, 1, \dots, 6)$ are constant parameters composed of initial conditions, time interval parameter t_k, t_{k+1} and design parameter $\dot{\Theta}_d^{\{k\}}(t_{k+1})$. The images of target trajectory (36) and time derivative of them are shown in Fig.6. Remark

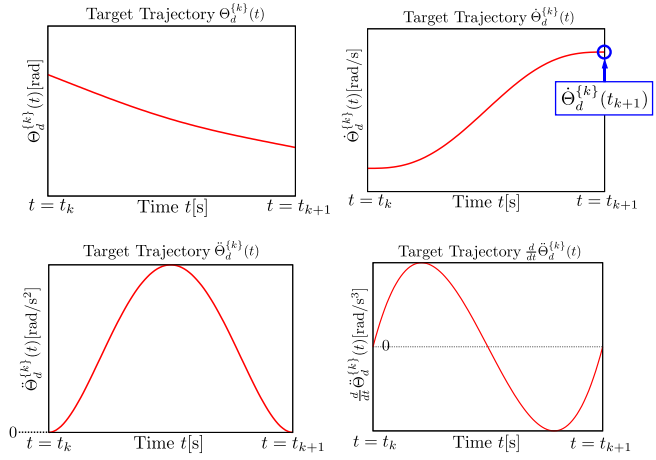


Fig. 6. Property of Target Time Trajectory $\Theta_t(t, t_f, \dot{\Theta}_t(t_f))$

that maintaining the achievement of 1st step is always realized by updating $\Theta_d^{\{k\}}(t)$ designed in (36) at each interval k .

Next, let challenge (b) be discussed. Since t_{k+1} and $\dot{\Theta}_d^{\{k\}}(t_{k+1})$ can be arbitrarily chosen, these design parameter can be interpreted as the input to zero dynamics. Hence, let $\dot{\Theta}_d^{\{k\}}(t_{k+1})$, the one of the virtual inputs to zero dynamics, denote u_v . The virtual input u_v can be the input to the discretized zero dynamics at interval k . This is expressed by

$$\dot{\zeta}[k+1] = \Gamma(\mathbf{O}^{9 \times 1}, \zeta[k], u_v) \quad (37)$$

. Note that (37) is the discretized system of (34).

If the discrete dynamical system (37) is analytically derived, the controller can be analytically designed. However, in this case of 15 dimensional UAV model, the zero dynamics is too complicated to find the analytical solution. Therefore, the design of virtual input u_v is designed to be PID control against the error e as is shown in

$$u_v = \dot{\Psi}(t_k) + K_p e + K_i \int_{t_0}^{t_k} e dt \quad (38)$$

. Note that this would not analytically guarantee the stability.

D. Numerical Simulation

In this numerical simulation, it is assumed that all of states can be measured by sensors. The model parameters used in this simulation are given in Table III and Table IV. In addition, symmetric property is assumed against $\mathbf{J}_r, \mathbf{D}_r$ and properties of propellers. In order to show the effect of the proposed controller, the 1st step is only focused at $0 \leq t < 5$. Here, the feedback input v in (25) is designed by LQ regulator. Then, the 2nd step is considered at $t \geq 5$. The

TABLE III
MODEL PARAMETER

m :	mass of robot	: 0.30 [kg]
$ r_i $:	distance between COG and rotor	: 0.15 [m]
g :	gravitational acceleration	: 9.8 [kgm ²]

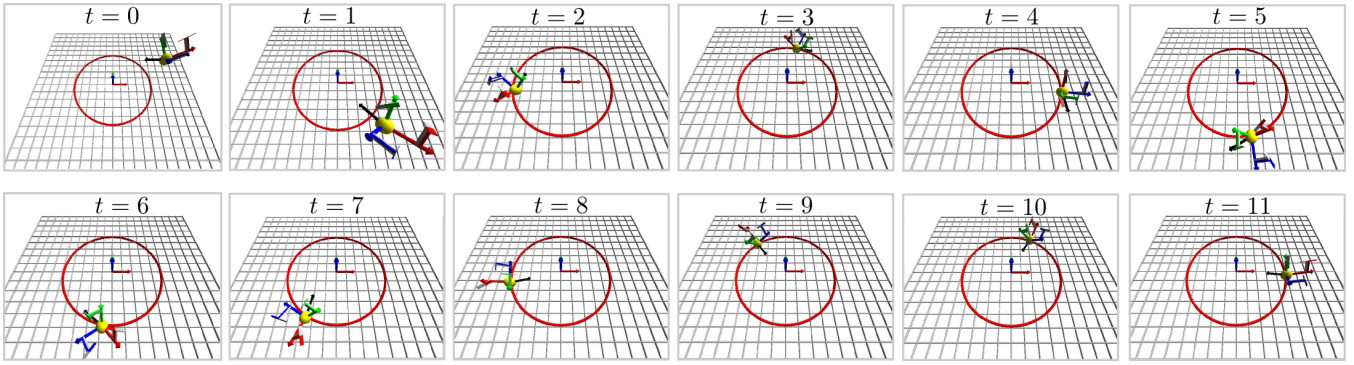


Fig. 7. Sequence of the Circle Motion Control with $\psi = \Theta$

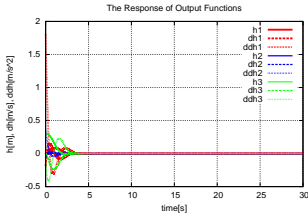


Fig. 8. time response of \mathbf{h}

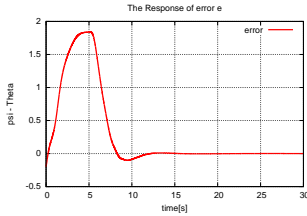


Fig. 9. error $e = \Psi - \Theta$

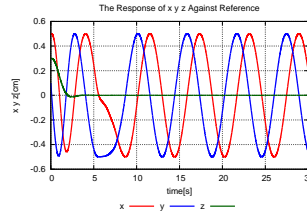


Fig. 12. position ξ

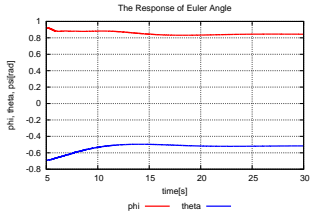


Fig. 13. attitude ϕ and θ

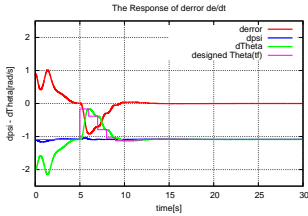


Fig. 10. \dot{e} and $\dot{\Theta}_d^{\{k+1\}}(t)$

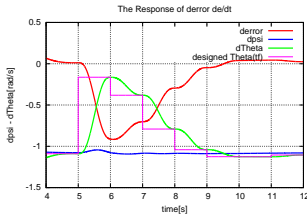


Fig. 11. details of Fig.10

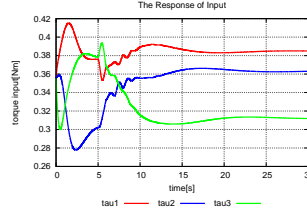


Fig. 14. input τ

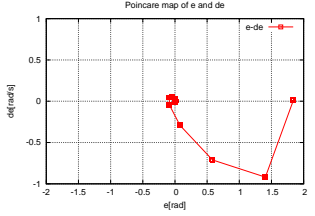


Fig. 15. e and \dot{e} at t_k in 2nd step

design parameter for the controller is also shown in Table IV. Remark that K_p and K_i is designed conservatively.

First, the sequence of movie of this numerical simulation is shown in Fig.7. This figure briefly confirms that certain point of UAV which is indicated by black arrow in Fig.7 faces to the center of a circular orbit while COG moves on circular orbit.

Second, the result of 1st step is shown in Fig.8. The linear subsystem is stabilized within 5 seconds. This confirms that the orbit of UAV is constrained on the circular orbit, meaning that the goal of 1st step is achieved.

Third, other graphs confirms the validity of the proposed discrete output zeroing control in 2nd step. Fig.9 shows the correspondance of rotation angle Ψ and revolution angle Θ , meaning the goal of 2nd step is achieved as well. This result shows that a certain state of zero dynamics is explicitly controlled by the suggested discrete output zeroing control, because time responses of output functions are kept to be zero at $t \geq 5$. Moreover, the performance of discrete controller is also shown in Fig.10 and Fig.11. The desired velocity of revolution angle $\dot{\Theta}_d^{\{k+1\}}(t)$ is smoothly updated. Finally, Poincaré map of $e - \dot{e}$ plane at each interval k is shown in Fig.15. The stability of the controller (38) is

numerically confirmed.

V. CONCLUSIONS AND FUTURE WORKS

In this paper, we proposed the controller design to realize circle motion with the attitude control via discrete output zeroing control for UAV having three inputs. The control strategy is based on two steps. As a first step, COG of UAV is focally controlled on a circular orbit. As a second step, the discrete output functions are designed to keep continuity in the boundary in order to maintain achievement of the control objective in first step. Finally, the numerical simulation verified the validity of the proposed controller. As

TABLE IV
CONTROLLER PARAMETERS

(x_r, y_r)	: desired center of a circular orbit:	(0, 0) [m]
z_r	: desired height	: 0 [m]
r	: radius of a circular orbit	: 0.5 [m]
\mathbf{Q}	: \mathbf{Q} matrix of LQ gain	: $\text{diag}\{\mathbf{1}^{1 \times 6}, 100.0, 1.0, 1.0\}$
\mathbf{R}	: \mathbf{R} matrix of LQ gain	: $\mathbf{I}^{3 \times 3}$
$t_{k+1} - t_k$: time interval of update	: 1.0 [s]
K_p	: proportional gain in (38)	: 0.01
K_i	: integral gain in (38)	: 0.001

a conclusion, circle motion can be obtained by three inputs even though hovering control can not be realized.

Proof of stability of the rest of zero dynamics, e.g. ϕ and θ shown in Fig.13, remains as a future work.

REFERENCES

- [1] Y. Kataoka, K. Sekiguchi and M. Sampei, *Nonlinear Control and Model Analysis of Trirotor UAV Model*, Proc. of the 18th Int. Federation of Automatic Control World Congress, 2011
- [2] M. Ishikawa and M. Sampei, *On Equilibria Set and Feedback Stabilizability of Nonlinear Control Systems*, Proc. of International Federation of Automatic Control Symposium on Nonlinear Control Systems Design, 1998. pp 637–642.
- [3] Gabriel M. Hoffmann, Huang, H. , Steven L. Waslander and Claire J. Tomlin, *Quadrotor Helicopter Flight Dynamics and Control: Theory and Experiment*, Proc. of AIAA Guidance, Navigation and Control Conference and Exhibit, 2007
- [4] S. Salazar-Cruz, F. Kendoul, R. Lozano and I. Fantoni, *Real-Time Control of a Small-Scale Helicopter Having Three Rotors*, Proc. of IEEE Int. Conf. on Intelligent Robots and Systems, 2006, pp 2924–2929.
- [5] P. Fan, X. Wang and K. Cai, *Design and Control of a Tri-Rotor Aircraft*, Proc. of IEEE Int. Conf. on Control and Automation, 2010, pp 1972-1977.
- [6] Alberto Isidori, *Nonlinear Control Systems, Second Edition*, Springer, 1999
- [7] A.M. Bloch, *Nonholonomic Mechanics and Control*, 1st ed., Springer, 2003.